eChem
https://www.sciltp.com/journals/eChem

Supplementary Materials

Atomically Precise Ag_9Cu_6 and Ag_{15} Nanoclusters for Nitrate Electroreduction to NH_3: Probing the Cu Doping Effect

Jiaming Tan [1,†], Yingwei Li [2,*,†], Liang Qiao [3,†], Jingwen Yang [1], Tao Wu [1], Lubing Qin [1], Ruihao Huang [1], Chunsheng Yang [3], Kebin Chi [3,*] and Zhenghua Tang [1,*]

[1] New Energy Research Institute, School of Environment and Energy, South China University of Technology, Guangzhou Higher Education Mega Centre, Guangzhou 510006, China
[2] Department of Chemistry, University of Hawai'i at Manoa, Bilger 321A, 2545 McCarthy Mall, Honolulu, HI 96822, USA
[3] Petrochemical Research Institute, PetroChina Company Limited, Beijing 102206, China
* Correspondence: yingweil@hawaii.edu (Y.L.); ckb459@petrochina.com.cn (K.C.); zhht@scut.edu.cn (Z.T.)
† These authors contributed equally to this work.

How To Cite: Tan, J.; Li, Y.; Qiao, L.; et al. Atomically Precise Ag_9Cu_6 and Ag_{15} Nanoclusters for Nitrate Electroreduction to NH_3: Probing the Cu Doping Effect. *eChem* **2026**, *2*(1), 6. https://doi.org/10.53941/echem.2026.100006

1. Chemicals and Materials

Methanol (MeOH, HPLC grade), ethanol (HPLC grade) dichloromethane (DCM, HPLC grade), acetonitrile (MeCN, HPLC grade), ethyl acetate (HPLC grade), *n*-hexane (HPLC grade), silver trifluoroacetate (CF_3CO_2Ag, 98%), sodium methoxide (CH_3ONa, 95%), 3, 3-dimethyl-1-butyne (^{t}Bu-C≡CH, 98%), aqueous ammonia (28% NH_3 in H_2O), sodium cyanoborohydride ($NaBH_3CN$, 98%), Sodium hexafluoroantimonate ($NaSbF_6$), potassium hydroxide (KOH, 95%), sodium nitrate ($NaNO_3$, 99%), salicylic acid (98%), sulfanilic acid (99%), sodium citrate (98%), sodium hydroxide (NaOH, 95%), sodium nitroferricyanide dihydrate ($Na_2[Fe(CN)_5NO]\cdot 2H_2O$, 97%), potassium nitrite (KNO_2, 96%), potassium nitrate (KNO_3, 99%), sodium hypochlorite (NaClO, 98%), ammonium chloride (NH_4Cl, >99.9%), *N*-(1-naphthyl)ethylenediamine dihydrochloride ($C_{10}H_7NHC_2H_4NH_2\cdot 2HCl$, 98%), sulfanilamide (98%), phosphoric acid (H_3PO_4, 99%), hydrochloric acid (HCl, 37%), hydrophobic carbon cloth were all purchased from Energy Chemical (Shanghai, China). $NaNO_3$ (99.5%), ether (99%), and hydrochloric acid (99%) were bought from Guangzhou Dongzheng Chemical Reagent (Guangzhou, China). The water with the resistivity of 18.3 MΩ·cm was supplied by a Barnstead Nanopure water system. All chemicals were used as received without further treatment.

2. Preparation of Ag_{15} and Ag_9Cu_6 Nanoclusters

$Ag_{15}(C{\equiv}C^tBu)_{12}^+$

In a typical procedure, solution A containing 136 mg CF_3CO_2Ag in 15 mL dichloromethane and 1 mL acetonitrile, solution B containing 83 mg CH_3ONa and ^{t}BuC≡CH (15 μL) in 2 mL methanol, solution C containing 144 mg $NaBH_3CN$ in 10 mL MeOH were prepared separately. Under vigorous stirring, solution B was added into solution A to yield a colorless suspension, followed by the rapid injection of solution C. An immediate color transition to purple was observed, indicating the formation of NCs. The reaction was kept in an ice bath for 3 h. Then, the solvent was removed via rotary evaporation, and the crude solid was extracted and purified using a DCM/acetonitrile mixture to give Ag_{15} as a purple solution.

$Ag_9Cu_6(C{\equiv}C^tBu)_{12}^+$

To get ^{t}BuC≡CAg(I) precursor, Ag_2O (500 mg, 2.1 mmol) was suspended in 20 mL of aqueous ammonia and kept vigorously stirring for 10 min until complete dissolution. After filtration, 5 mL of deionized water was added into the filtrate and ^{t}Bu-C≡CH (950 mg, 4.1 mmol in 2.5 mL of ethanol) was added dropwise under vigorous stirring (1000 rpm) over 10 min. The white precipitate was washed repeatedly with deionized water, ethanol, and diethyl ether, and collected via centrifugation to yield ^{t}BuC≡CAg(I). In a typical synthesis of $Ag_9Cu_6(C{\equiv}C^tBu)_{12}^+$, ^{t}BuC≡CAg(I) (6.30 mg, 0.03 mmol) and $NaSbF_6$ (7.84 mg, 0.03 mmol) were ultrasonically co-dispersed in 4 mL DCM and 2 mL MeCN at room temperature. After 10 min, a freshly prepared solution of $(PPh_3)_2CuBH_4$ was added

under vigorous stirring for an additional 10 min. The solution color changed from colorless to yellow and eventually to dark brown. The mixture was incubated for 12 h in the absence of light. The solvent was removed via rotary evaporation and the dark solid was washed with ethyl acetate and methanol extensively. $Ag_9Cu_6(C{\equiv}C^tBu)_{12}^+$ were then extracted with DCM to give a blue solution.

3. Electrochemical Measurements

The catalyst ink was prepared by homogeneously dispersing the catalyst in a mixture of ethanol and a Nafion solution. To prepare the catalytic composite, the as-prepared NC was immobilized onto XC-72 carbon black at a mass ratio of 2: 1 (10 mg NC: 5 mg carbon black). The catalyst ink precursor was obtained by dispersing the composite in ethanol (1.5 mg mL^{-1}) via sonication for 30 min. The final catalyst ink was formulated by uniformly mixing 1 mL of the above suspension with 40 μL of 5 wt.% Nafion solution. Subsequently, 120 μL of the ink was uniformly drop-cast onto a hydrophobic carbon cloth substrate to yield a working electrode with a geometric area of 1 × 1 cm^2. Electrochemical evaluation was conducted on a computer-controlled Donghua electrochemical workstation utilizing a standardized three-electrode architecture. A Pt plate (1 × 1 cm^2) and a Hg/HgO electrode (filled with 1.0 M KOH) were employed as the counter and reference electrodes, respectively. The anodic and cathodic compartments of the typical H-type cell were separated by a Nafion 117 membrane, which had been sequentially pretreated at 80 °C in a 5% H_2O_2 aqueous solution for 1 h and in deionized water for another 1 h. All measured potentials were normalized to the reversible hydrogen electrode (RHE) scale.

$$E_{\mathrm{RHE}} = E_{\mathrm{Hg/HgO}} + 0.0591 \times \mathrm{pH} + 0.098$$

Electrocatalytic NO_3RR Evaluation

The NO_3RR performance was investigated in a 1 M KOH + 0.1 M KNO_3 electrolyte under continuous mass transport regulated by mechanical stirring at 300 rpm. Prior to and during the electrochemical tests, the dissolved oxygen/air in the catholyte was strictly eliminated via continuous inert gas purging. Linear sweep voltammetry (LSV) curves were acquired at a scan rate of 10 mV s^{-1}, with an 80% iR–compensation applied to all polarization curves. To evaluate the ECSA, the electrochemical double–layer capacitance (C_{dl}) was measured via cyclic voltammetry (CV) within a non–Faradaic potential region of 0.34–0.46 V vs. RHE at scan rates ranging from 20 to 120 mV s^{-1}. The charging current density differences ($j_a - j_c$) displayed a linear relationship with the scan rates, where the linear slope is mathematically equivalent to 2 C_{dl}. The ECSA was subsequently calculated using the empirical relation:

$$\mathrm{ECSA} = C_{\mathrm{dl}}/C_{\mathrm{s}}$$

Potentiostatic investigations were automatically terminated upon capturing a total Coulombic charge of 800 C per interval. The electrocatalytic durability of the Ag_9Cu_6 catalyst was assessed at −0.6 V vs. RHE through 7 successive potentiostatic cycles, where each run was automatically terminated upon capturing a total Coulombic charge of 800 C. The electrocatalytic durability of the Ag_{15} catalyst was assessed at −0.5 V vs. RHE through 7 successive potentiostatic cycles, where each run was automatically terminated upon capturing a total Coulombic charge of 800 C.

4. Quantitative Detection

4.1. Quantification of NH_3

The NH_3 concentration was determined using the indophenol blue spectrophotometric method. Three chromogenic reagents were prepared as follows: Reagent A, containing 5 g salicylic acid, 5 g sodium citrate, and 4 g NaOH dissolved in 100 mL of H_2O; Reagent B, containing 1 g $Na_2[Fe(CN)_5NO]{\cdot}2H_2O$ dissolved in 100 mL of H_2O; and Reagent C, containing 8.3 g NaClO dissolved in 100 mL of H_2O. For analysis, an electrolyte aliquot (3 mL) was sequentially mixed with 200 μL of Reagent B, 2 mL of Reagent A, and 1 mL of Reagent C. After incubation for 30 min, the absorbance was measured at 655 nm using a UV-vis spectrophotometer. A calibration curve was established using standard NH_4Cl solutions.

4.2. Quantification of Nitrite (NO_2^-)

The NO_2^- concentration was determined colorimetrically using a Griess-type reagent prepared from 0.2 g $C_{10}H_7NHC_2H_4NH_2{\cdot}2HCl$, 4 g sulfanilamide, and 10 mL H_3PO_4 in 50 mL H_2O. 100 μL of the reagent was added

into an electrolyte aliquot (5 mL). After standing for 30 min at room temperature, the absorbance was recorded at 540 nm using a UV-vis spectrophotometer. A calibration curve was established using standard KNO_2 solutions.

4.3. Quantification of Nitrate (NO_3^-)

The NO_3^- concentration was determined by UV-vis spectroscopy. 0.1 mL of 1.00 M HCl and 0.01 mL of 0.8 wt.% sulfanilic acid were added into an electrolyte aliquot (5 mL). After reacting for 30 min, the absorbance was recorded at 220 nm and 275 nm, respectively. The corrected absorbance was calculated according to the equation $A = A_{220\ nm} - 2A_{275\ nm}$. A calibration curve was established using standard KNO_3 solutions.

5. Theory/Calculation

The NH_3 yield rate and Faradaic efficiency was calculated by the following equations:

The NH_3 yield rate was calculated using the following Equation:

$$NH_3\ \text{yield rate} = \frac{C_{NH_3} \times V}{M_{NH_3} \times t \times A}$$

where C_{NH_3} is the concentration of NH_3 produced, V is the volume of the catholyte of the cathode chamber (30 mL), A is the geometric area of the working electrode (1 cm^2); t is the electrolysis time.

The Faradaic efficiency (FE) was calculated using the following Equation:

$$\text{Faradaic efficiency} = \frac{n \times c \times V \times F}{Q}$$

$$FENH_3 = \frac{8 \times F \times C_{NH_3} \times V}{M_{NH3} \times Q}$$

$$FENO_2^- = \frac{2 \times F \times C_{NO_2^-} \times V}{M_{NO_2^-} \times Q}$$

where C_{NH_3} represents the mass concentration of the generated NH_3 ($g \cdot L^{-1}$), $C_{NO_2^-}$ represents the mass concentration of the generated NO_2^- ($g \cdot L^{-1}$), V is the volume of the catholyte (L), $M_{NO_2^-}$ denotes the molar mass of NO_2^- ($g \cdot mol^{-1}$), and M_{NH_3} denotes the molar mass of NH_3 ($g \cdot mol^{-1}$). T corresponds to the electrolysis duration (h). Furthermore, n defines the number of transferred electrons required for the specific reduction pathway, F is the Faraday constant (96,485 $C \cdot mol^{-1}$), and Q signifies the total integrated charge accumulated during the electrocatalytic process (C).

Table S1. The comparison between Ag_9Cu_6 and other catalysts in eNO_3RR.

Catalyst	FE_{NH_3}	NH_3 Yield Rate	Nitrate Concentration	pH	Potential (V vs. RHE)	
Ag_9Cu_6	88.48	9.93 $mg \cdot h^{-1} \cdot cm^{-2}$	0.1 M	14	−0.6	This work
$Ag_{20}Cu_{12}$ NCs	84.6	0.138 $mmol \cdot h^{-1} \cdot cm^{-2}$	0.1 M	14	−0.8	[1]
$Ag_{13}Cu_4$ NCs	90.4	0.215 $mmol \cdot h^{-1} \cdot cm^{-2}$	0.1 M	14	−0.7	[2]
Defect-rich Cu nanoparticles	99.7	0.89 $mmol \cdot h^{-1} \cdot cm^{-2}$	0.02 M	14	−0.4	[3]
Defective Cu nanowire arrays	>90	7.85 $mmol \cdot h^{-1} \cdot cm^{-2}$	100 mM	7	−0.3	[4]
Bimodal nanoporous Ag/Ag-Co	97.1	25.1 $mg \cdot h^{-1} \cdot cm^{-2}$	50 mM	14	−0.6	[5]
$Ag@Cu_3N$/CF	95.9	1.91 $mmol \cdot h^{-1} \cdot cm^{-2}$	0.1 M	14	−0.3	[6]
Cu/Ag-Ru/C	93.5	3.45 $mmol \cdot h^{-1} \cdot cm^{-2}$	0.5 M	14	−0.9	[7]
CuAgTe NWs	98.3	8.30 $mg \cdot h^{-1} \cdot cm^{-2}$	0.1 M	14	−0.5	[8]
AgCu NWs	95.5	2.56 $mg \cdot h^{-1} \cdot cm^{-2}$	50 mg/L	7	−0.6	[9]
$Cu_{11}Ag_3$ nanotips	98.8	2.36 $mmol \cdot h^{-1} \cdot cm^{-2}$	1800 mg/L	14	−0.33	[10]
Ag/Cu/MXene	87.7	10.3 $mol \cdot h^{-1} \cdot g^{-1}$	0.1 M	14	−1	[11]

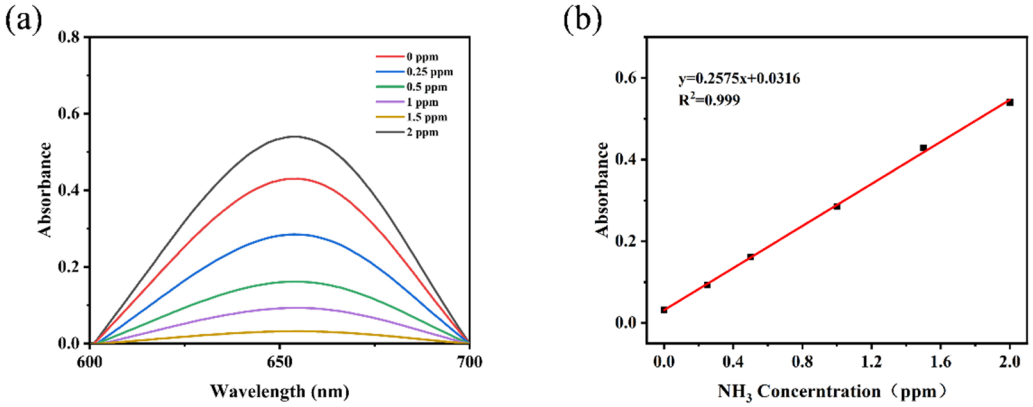

Figure S1. (**a**) The UV-vis absorption spectra for standard $(NH_4)_2SO_4$ solutions with different concentrations in 1 M KOH and (**b**) corresponding calibration curve for the colorimetric NH_4^+ assay.

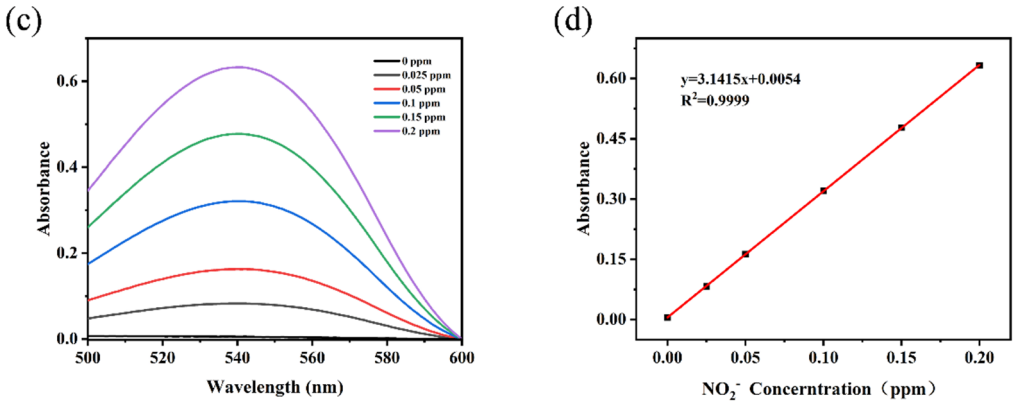

Figure S2. (**a**) The UV-vis absorption spectra for standard KNO_2 solutions with different concentrations in 1 M KOH and (**b**) corresponding calibration curve for the colorimetric NO_2^- assay.

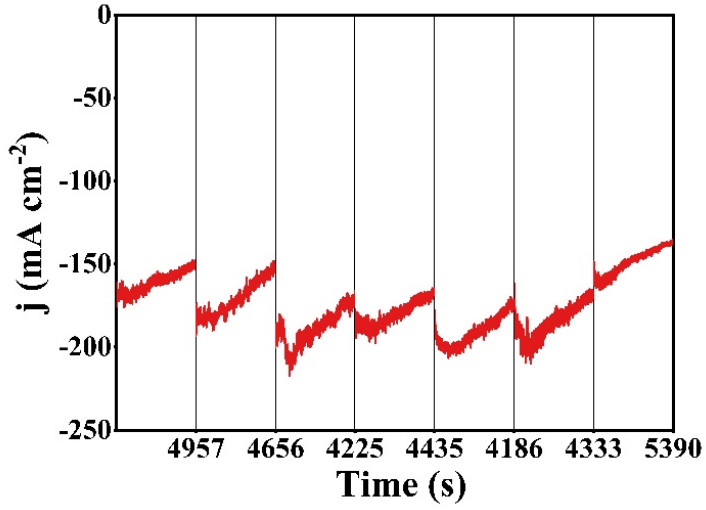

Figure S3. Chronoamperometric responses (current density vs. time) of Ag_9Cu_6 under potentiostatic conditions at an applied potential of −0.6 V vs. RHE. All measurements were conducted until the total charge transferred amounted to 800 C.

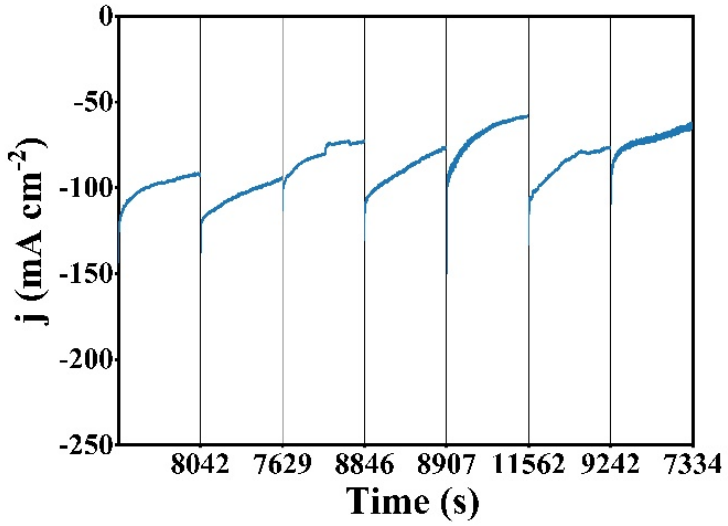

Figure S4. Chronoamperometric responses (current density vs. time) of Ag_{15} under potentiostatic conditions at an applied potential of −0.6 V vs. RHE. All measurements were conducted until the total charge transferred amounted to 800 C.

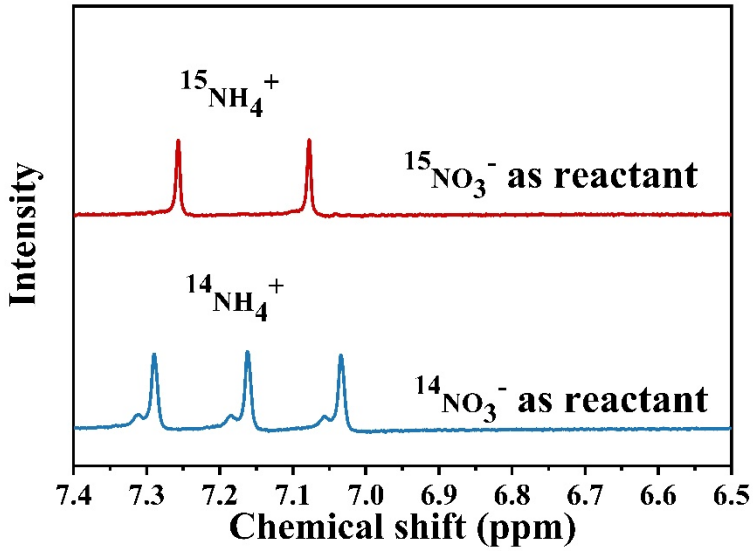

Figure S5. ^{1}H NMR spectra of eNO_3RR using Ag_9Cu_6 as catalysts and $^{15}NO_3^-$ or $^{14}NO_3^-$ as electrolytes.

References

1. Ma, G.; Sun, F.; Qiao, L.; et al. Atomically Precise Alkynyl-Protected $Ag_{20}Cu_{12}$ Nanocluster: Structure Analysis and Electrocatalytic Performance toward Nitrate Reduction for NH_3 Synthesis. *Nano Res.* **2023**, *16*, 10867–10872.
2. Wang, J.; Cai, J.; Ren, K.-X.; et al. Stepwise Structural Evolution toward Robust Carboranealkynyl-Protected Copper Nanocluster Catalysts for Nitrate Electroreduction. *Sci. Adv.* **2024**, *10*, eadn7556.
3. Liu, X.; Liu, J.; Chen, A.; et al. 99.7% Faradaic Efficiency in Nitrate Reduction Enabled by Defect-Rich Copper Nanoparticles. *ACS Appl. Nano Mater.* **2025**, *8*, 17518–17526.
4. Zhang, B.; Dai, Z.; Chen, Y.; et al. Defect-Induced Triple Synergistic Modulation in Copper for Superior Electrochemical Ammonia Production across Broad Nitrate Concentrations. *Nat. Commun.* **2024**, *15*, 2816.
5. Feng, Z.; He, Y.; Cui, Y.; et al. Efficient Tandem Electrocatalytic Nitrate Reduction to Ammonia on Bimodal Nanoporous Ag/Ag–Co across Broad Nitrate Concentrations. *Nano Lett.* **2024**, *24*, 11929–11936.
6. Dong, H.; Ye, J.; Liu, X.; et al. Spatially Separated Ag@Cu_3N Tandem Electrocatalyst with High Nitrate-to-Ammonia Selectivity via Decoupled Deoxygenation-Hydrogenation Pathway. *Adv. Funct. Mater.* **2025**, *35*, e26882.
7. Jia, R.; Zhang, X.; Gan, L.; et al. Boosting Electrocatalytic Nitrate Reduction to Ammonia with a Cu/Ag-Ru Tandem Catalyst at Industrial-Scale Current Density. *J. Mater. Chem. A* **2025**, *13*, 5732–5743.

8. Meng, Z.; Wang, S.; Li, Y.; et al. Tandem Catalysis Facilitates Nitrate-to-Ammonia Electroreduction on AgCu Telluride Nanowires. *Sci. China Chem.* **2026**, *69*, 2331–2337.
9. Liu, X.; Xiang, T.; Liu, J.; et al. Ag Single Atoms Boosting Water Dissociation on Cu Nanowires for Efficient H-Mediated Nitrate Reduction at Ultra-Low Concentrations with Ammonia Recovery. *Adv. Funct. Mater.* **2026**, *36*, e241402.
10. Qin, L.; Sun, F.; Gong, Z.; et al. Electrochemical NO_3^- Reduction Catalyzed by Atomically Precise $Ag_{30}Pd_4$ Bimetallic Nanocluster: Synergistic Catalysis or Tandem Catalysis? *ACS Nano* **2023**, *17*, 12747–12758.
11. Kui, B.; Zhao, S.; Hu, Y.; et al. Strongly Coupled Ag/Cu with MXene for Efficient Tandem Nitrate Reduction Reaction and Zinc–Nitrate Batteries. *Catal. Sci. Technol.* **2025**, *15*, 1617–1626.